Please cite this article as:
Ewa Węgrzyn-Skrzypczak, Tomasz Skrzypczak, Mathematical and numerical model of 3D natural convection in a cube, Scientific Research of the Institute of Mathematics and Computer Science, 2009, Volume 8, Issue 1, pages 185-191.
The website: http://www.amcm.pcz.pl/

MATHEMATICAL AND NUMERICAL MODEL OF 3D NATURAL CONVECTION IN A CUBE

Ewa Węgrzyn-Skrzypczak, Tomasz Skrzypczak

Institute of Mathematics, Czestochowa University of Technology, Poland
skrzyp@imipkm.pcz.czest.pl

Abstract. In the paper mathematical and numerical model of air convection in 3D region is considered. Governing equations of the model are presented. Main assumptions of numerical approach are discussed. Finite Element Method (FEM) with Characteristic Based Split (CBS) scheme is used to solve the problem. Two examples of numerical calculation are presented and discussed.

Introduction

Natural convection is a phenomenon in which the fluid motion is not generated by any external source (like a pump, fan, suction device etc.) but only by density differences in the fluid induced by temperature gradients. In natural convection, fluid receives heat in the vicinity of a heat source, becomes less dense and rises. The surrounding, lower-temperature fluid then moves to replace it. This cooler fluid is then heated and the process continues leading to convection cells formation. This process also transfers heat energy from the bottom of the convection cell to top. The driving force for natural convection is buoyancy, a result of differences in fluid density.

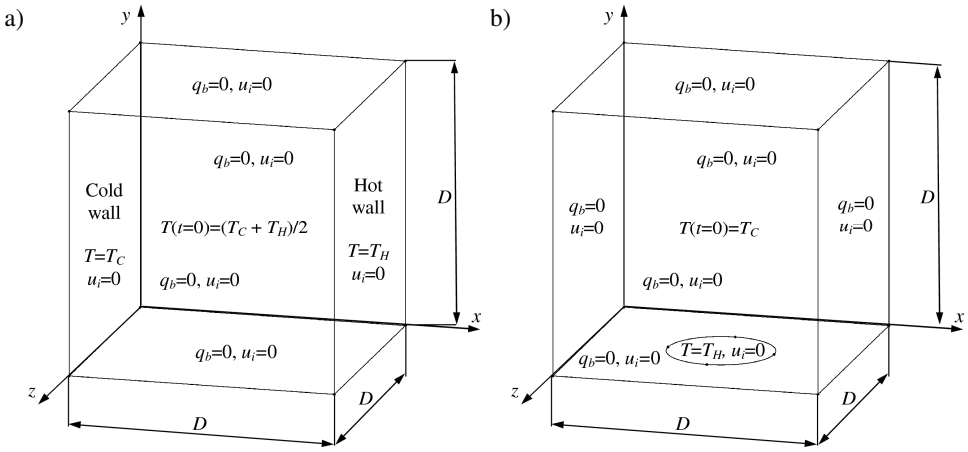

Fig. 1. The geometry, the boundary and initial conditions of the problem

Natural convection in a differential sidewall-heated air-filled enclosure is a basic model for simulating various classes of thermal engineering systems [1]. For two past decades a large number of investigations have been conducted, mostly for two-dimensional enclosures. A set of benchmark solutions was proposed for various Rayleigh number $10^3 \div 10^6$ for a two-dimensional square cavity for which horizontal walls are insulated [2].

Presented paper examines numerically the effect of the thermal boundary conditions at the vertical walls ($x = 0$ and 0.1 m) on the characteristics of three-dimensional fields in a differentially heated cubical enclosure (Fig. 1a), while other walls are thermally insulated. Additionaly numerical simulation was performed with circular heated region on the bottom wall while the others were insulated (Fig. 1b).

1. Mathematical model

The flow is governed by the time-dependent, incompressible Navier-Stokes (1) and energy equations (2). The Boussinesq approximation is invoked for the fluid properties. Set of equations contains also a continuity equation (3).

$$\frac{\mu}{\rho} u_i{}_{,jj} - u_j u_i{}_{,j} - \frac{1}{\rho} p_{,i} - g_i \beta (T - T_{ref}) = \frac{\partial u_i}{\partial t} \tag{1}$$

$$c\rho \left(\frac{\partial T}{\partial t} + u_i T_{,i} \right) = (\lambda T_{,i})_{,i} \tag{2}$$

$$u_i{}_{,i} = 0 \tag{3}$$

where T [K] means temperature, u_i [m/s] is velocity component, t [s] - time, λ [W/(mK)] - thermal conductivity, μ [kg/ms] - dynamic viscosity, c [J/(kgK)] - specific heat, ρ [kg/m^3] - density, g_i [m/s^2] - acceleration component, β [K^{-1}] - volumetric thermal expansion coefficient, T_{ref} [K] indicates reference temperature.

Equations (1-3) are completed by the Dirichlet and Neumann boundary conditions

$$\mathbf{x} \in \Gamma_1 : T = T_b \tag{4}$$

$$\mathbf{x} \in \Gamma_2 : -\lambda \mathbf{n} \cdot \mathbf{grad} T = q_b \tag{5}$$

and following initial conditions

$$\mathbf{x} \in \Gamma_{1-3} : u_i = 0, \quad t = 0 : T = T_0, \quad u_i = 0 \tag{6}$$

$$t = 0 : T = T_0, \quad u_i = 0 \tag{7}$$

where T_b [K] is known boundary temperature, q_b [W/m^2] - heat flux normal to the boundary, T_0 [K] - initial temperature.

2. Numerical model

The weighted residual method [3] for the heat conductivity equation (1) is used

$$\int_{\Omega} w\left[\left(\lambda T_{,i}\right)_{,i} - c\rho\left(\frac{\partial T}{\partial t} + u_i T_{,i}\right)\right] d\Omega = 0 \tag{8}$$

Weak form of (9) is obtained

$$\int_{\Omega} \lambda w_{,i}\, T_{,i}\, d\Omega + \int_{\Omega} c\rho w u_i T_{,i}\, d\Omega + \int_{\Omega} c\rho w \frac{\partial T}{\partial t} d\Omega = \oint_{\Gamma} w q_b d\Gamma \tag{9}$$

The above equation is discretized over space using Petrov-Galerkin method [4-6]. For the single finite element one can write

$$\begin{aligned} \lambda^e \int_{\Omega^e} w_{i,k}\, N_{j,k}\, d\Omega + (c\rho)^e \int_{\Omega^e} w_i N_j u_k^j N_{l,k}\, d\Omega + \\ + (c\rho)^e \int_{\Omega^e} w_i N_j d\Omega = \oint_{\Gamma^e} w_i q_b d\Gamma \end{aligned} \tag{10}$$

where N_i is linear shape function of the finite element and w_i [4] can be written as follows

$$w_i = N_i + \gamma_i \frac{h_i}{2} \frac{\left(u_k^i N_{i,k}\right)}{\left|u^i\right|} \tag{11}$$

where h_i is element size in the direction of velocity vector [7], γ_i and Peclet number $P_e^{\,i}$ are calculated using following formulas

$$\gamma_i = \operatorname{ctgh}\left(P_e^i\right) - \frac{1}{P_e^i} \tag{12}$$

$$P_e^i = \frac{c\rho\left|u^i\right| h_i}{2\lambda} \tag{13}$$

Integral terms from (10) can be written in the following matrix form

$$\begin{aligned} K_{ij}^e = \lambda^e \int_{\Omega^e} w_{i,k}\, N_{j,k}\, d\Omega, \quad A_{ij}^e = (c\rho)^e \int_{\Omega^e} w_i N_j u_k^l N_{l,k}\, d\Omega \\ M_{ij}^e = (c\rho)^e \int_{\Omega^e} w_i N_j d\Omega, \quad B_{ij}^e = \oint_{\Gamma^e} w_i q_b d\Gamma \end{aligned} \tag{14}$$

where: $\mathbf{K}^e$ is element heat conductivity matrix, $\mathbf{A}^e$ - advection matrix, $\mathbf{M}^e$ - heat capacity matrix and $\mathbf{B}^e$ - right hand side vector.

After procedure of discretization over time (Euler backward scheme) and agregation of the discrete model we obtain global finite element equation

$$\left(\mathbf{K}+\mathbf{A}+\frac{1}{\Delta t}\mathbf{M}\right)\mathbf{T}^{f+1}=\frac{1}{\Delta t}\mathbf{M}\mathbf{T}^{f}+\mathbf{B} \tag{15}$$

We solve momentum equation (1) with use of characteristic based split (CBS) scheme which is based on the projection method of Chorin [8] as described in Zienkiewicz and Codina [9] and Zienkiewicz and Taylor [10]. In this method an auxiliary velocity field $\mathbf{u}^*$ is introduced to uncouple equations (1) and (3)

$$\begin{aligned}\Delta u_i^* = u_i^* - u_i^f = \Delta t\Bigg[&\frac{\mu}{\rho}u_{i,jj} - u_j u_{i,j} - g_i\beta(T-T_{ref}) + \\ &+\frac{\Delta t}{2}u_k\left[u_j u_{i,j} + g_i\beta\left(T-T_{ref}\right)\right]_k\Bigg]_{t=t^f}\end{aligned} \tag{16}$$

The final velocity field is corrected by the pressure increment so that is divergence free

$$u_i^{f+1} - u_i^* = -\frac{\Delta t}{\rho}\left(p_{,i}\right)^{f+1} \tag{17}$$

By taking the divergence of (17) we arrive at the following Poisson equation for the pressure

$$\Delta t\left(p_{,ii}\right)^{f+1} = \rho u_{i,i}^* \tag{18}$$

We apply the standard Galerkin procedure for (16-18).

2. Example of calculations

Computer program using finite element method has been made on the base of theoretical assumptions. Finite element mesh was created with use of GMSH generator. It contained 75434 nodes and 422873 tetrahedrons. Considered region was filled with air. Material properties used in calculations are shown in Table 1.

Rayleigh and Prandtl number of the flow was calculated with use of following relations

$$\mathrm{Ra} = \frac{\beta g (T_H - T_C) D^3 \rho^2 c}{\mu \lambda} \tag{19}$$

$$\mathrm{Pr} = \frac{\mu c}{\lambda} \tag{20}$$

Table 1. Material properties of air

Material property	Value
λ [W/(mK)]	2.7e-2
ρ [kg/m^3]	1.1e-0
c [J/kg]	1.0e-3
μ [kg/(ms)]	1.9e-5
β [1/K]	3.3e-3

Calculations were made at Ra = 10^6 and Pr = 0.7. During the first case of calculation left vertical wall (x = 0 m) was cold (T_C = 0 K) and right vertical wall (x = = 0.1 m) was hot (T_H = 13.096 K). Other walls were insulated. In the second one all walls were insulated except of circular region of radius r = 0.02 m located in the centre of the bottom wall (y = 0 m) which was heated up to T_H.

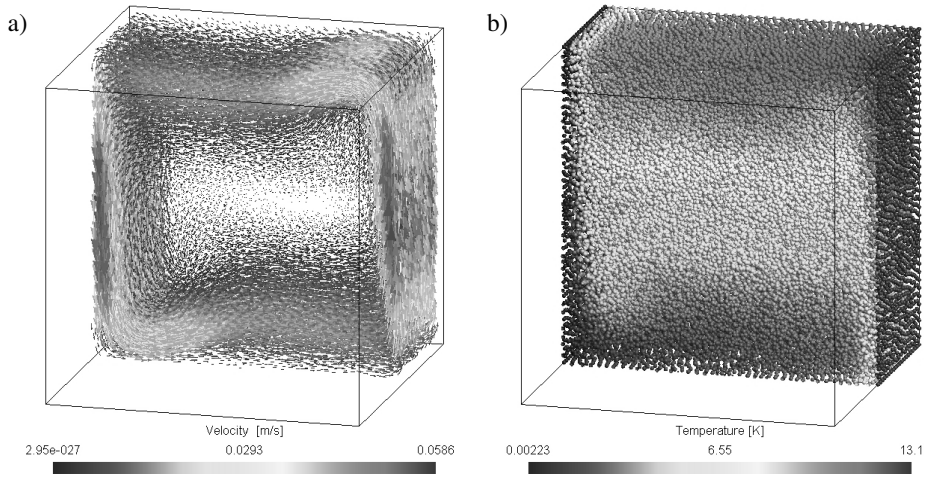

Fig. 2. Velocity (a) and temperature (b) of the air (1st case of calculation) after 18 s

The velocity and temperature field obtained from first case of calculation are displayed in Figure 2. At this Rayleigh number, the fields can be characterized by the presence of thin thermal and hydrodynamic boundary layers near the isothermal walls and an almost-stagnant central core. The heat transfer at the isothermal walls is reduced due to insulation of horizontal walls.

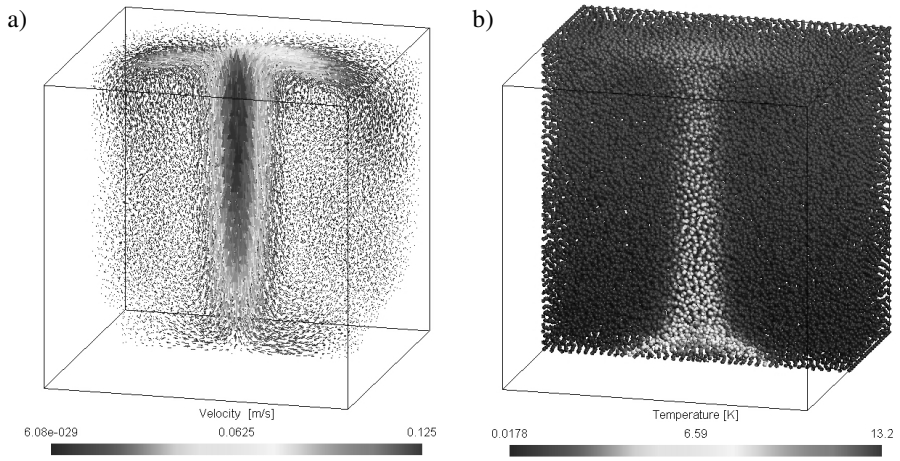

Fig. 3. Velocity (a) and temperature (b) of the air (2nd case of calculation) after 12 s

The velocity and temperature field in the second case are displayed in Figure 3. Symmetrical pattern of flow is showed in Figure 3a. Stream of the hot air moves up from the bottom to the top, where it forms characteristic shape. It well corresponds to temperature field showed in Figure 3b.

Conclusions

Presented mathematical and numerical model of the 3D non-isothermal flow in the cube is the base of further work. It will focus on modelling solidification of binary alloys process with motion of the liquid phase and shrinkage cavities formation.

References

[1] Ostrach S., Natural convection in enclosures, Journal of Heat Transfer 1988, 110, 1175-1190.

[2] De Vahl Davis G., Natural convection of air in a square cavity: a benchmark numerical solution, Int. J. Num. Methods Fluids 1983, 3, 249-264.

[3] Bathe K.J., Finite element procedures in engineering analysis, Prentice-Hall, Englewood Cliffs 1982.

[4] Svoboda Z., The analysis the convective-conductive heat transfer in the building constructions, Proceedings of the 6th Building Simulation Conference, Kyoto 1999, 1, 329-335.

[5] Hughes T.J.R., Recent progress in the development and understanding of SUPG methods with special reference to the compressible Euler and Navier-Stokes equations, International Journal for Numerical Methods in Fluids 1987, 7, 1261-1275.

[6] Bokota A., Kulawik A., Three dimensional model of thermal phenomena determined by moving heat source, Archives of Foundry 2002, 2(4), 74-79.

[7] Zienkiewicz O.C., Taylor R.L., The finite element method, 3: Fluid dynamics, Butterworth and Hienemann 2000.

[8] Chorin A.J., Numerical solution of the Navier-Stokes equation, Math. Comput. 1968, 23, 745--762.

[9] Zienkiewicz O.C., Codina R., A general algorithm for compressible and incompressible flow, Part I. The split characteristic based scheme, International Journal for Numerical Metods in Fluids 1995, 20, 869-885.

[10] Zienkiewicz O.C., Taylor R.L., The finite element method, 3: Fluid dynamics, Butterworth and Hienemann 2000.